Effects of Fe$_2$P and Li$_3$PO$_4$ additives on the cycling performance of LiFePO$_4$/C composite cathode materials

She-huang Wu [a,*], Je-Jang Shiu [a], Jeng-Yu Lin [b]

[a] Department of Materials Engineering, Tatung University, 40, Changshan N. Rd., Sec. 3, Taipei 104, Taiwan
[b] Department of Chemical Engineering, Tatung University, 40, Changshan N. Rd., Sec. 3, Taipei 104, Taiwan

ARTICLE INFO

ABSTRACT

In this study, a solution method was employed to synthesize LiFePO$_4$-based powders with Li$_3$PO$_4$ and Fe$_2$P additives. The composition, crystalline structure, and morphology of the synthesized powders were investigated by using ICP-OES, XRD, TEM, and SEM, respectively. The electrochemical properties of the powders were investigated with cyclic voltammetric and capacity retention studies. The capacity retention studies were carried out with LiFePO$_4$/Li cells and LiFePO$_4$/MCMB cells comprised LiFePO$_4$-based materials prepared at various temperatures from a stoichiometric precursor. Among all of the synthesized powders, the samples synthesized at 750 and 775 °C demonstrate the most promising cycling performance with C/10, C/5, C/2, and 1C rates. The sample synthesized at 775 °C shows initial discharge capacity of 155 mAh g^{-1} at 30 °C with C/10 rate. From the results of the cycling performance of LiFePO$_4$/MCMB cells, it is found that 800 °C sample exhibited higher polarization growth rate than 700 °C sample, though it shows lower capacity fading rate than 700 °C sample. For Fe$_2$P containing samples, the diffusion coefficient of Li$^+$ ion increases with increasing amount of Fe$_2$P, however, the sample synthesized at 900 °C shows much lower Li$^+$ ion diffusion coefficient due to the hindrance of Fe$_2$P layer on the surface of LiFePO$_4$ particles.
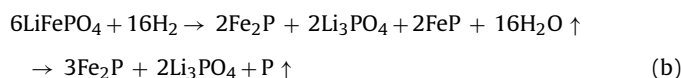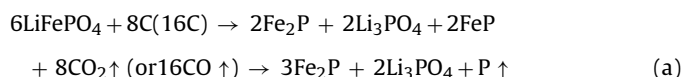
1. Introduction

Olivine-structured LiFePO$_4$ shows advantages of low cost, relative abundance of rough materials, small volume change during the charge/discharge process, and high thermal stability. Therefore, it has become the most promising cathode material for large scale lithium ion batteries as the power storage sources for use in hybrid electric vehicles (HEVs) and electric vehicles (EVs) [1]. However, LiFePO$_4$ is suffered from not only its poor electronic conductivity ($\sim$10^{-9} S cm^{-1}) but also the low mobility of Li$^+$ ions across the LiFePO$_4$/FePO$_4$ interface [2]. There are many methods that have been proposed to improve the electronic and ionic conductivity, such as carbon coating [3–6], morphology refinement [7,8], and metal ion doping [9–11].

It has been reported that additives, such as Fe$_2$P and Li$_3$PO$_4$, may also form in the LiFePO$_4$ samples while the temperature of heat treatment is higher than 800 °C or the reductive environment is employed [12]. Orthorhombic structured Li$_3$PO$_4$ has relatively low conductivity ($\sim$10^{-13} S cm^{-1} at 25 °C) which is even lower than that of LiFePO$_4$ ($\sim$10^{-9} S cm^{-1}), thus resulting in blocking the elec-

tron conduction between LiFePO$_4$ particles and decreasing the rate capability of the prepared LiFePO$_4$ sample [13,14]. On the contrary, it had been reported that Fe$_2$P networks at the surface of LiFePO$_4$ particles can enhance the electronic conductivity of LiFePO$_4$ sample due to the high conductivity of Fe$_2$P ($\sim$1.5 S cm^{-1}) [15]. Therefore, the existence of Fe$_2$P may be expected to improve the rate capability of LiFePO$_4$ materials [13,14,16–18]. In general, LiFePO$_4$ samples with hexagonal Fe$_2$P were prepared via a (a) carbothermal reduction or (b) hydrogen reduction [12].

$$6LiFePO_4 + 8C(16C) \rightarrow 2Fe_2P + 2Li_3PO_4 + 2FeP$$
$$+ 8CO_2\uparrow (or 16CO\uparrow) \rightarrow 3Fe_2P + 2Li_3PO_4 + P\uparrow \qquad (a)$$

$$6LiFePO_4 + 16H_2 \rightarrow 2Fe_2P + 2Li_3PO_4 + 2FeP + 16H_2O\uparrow$$
$$\rightarrow 3Fe_2P + 2Li_3PO_4 + P\uparrow \qquad (b)$$

In this study, olivine LiFePO$_4$ materials containing Fe$_2$P and Li$_3$PO$_4$ additives were prepared via a solution method by having a stoichiometric LiFePO$_4$ precursor heat-treated at various temperatures ranging from 700 to 900 °C. The effects of Fe$_2$P and Li$_3$PO$_4$ additives on the electrochemical properties of LiFePO$_4$ samples were investigated by cycling voltammetric analysis and capacity retention study.

* Corresponding author. Tel.: +886 2 25922458; fax: +886 2 25936897.
E-mail address: shwu@ttu.edu.tw (S.-h. Wu).

2. Experimental

Stoichiometric LiFePO$_4$ precursor was synthesized via a solution method by having iron powder (NC100.24, 99%, Hoganas, Sweden) dissolved in an aqueous citric acid (99.5%, Wako Pure Chem. Ind., Ltd., Japan) solution with iron: citric acid molar ratio of 1.0:0.25. Then, H$_3$PO$_4$ (85%, Wako Pure Chem. Ind., Ltd., Japan) and LiOH (95%, Wako Pure Chem., Ind., Ltd., Japan) were added into the solution with Li:Fe:P stoichiometric ratio of 1:1:1. 10 wt% of sucrose (Wako Pure Chem., Ind., Ltd., Japan) was added into the mixtures as a carbon source. After stirring for 4 h, the bath temperature was raised up to 65 °C to evaporate water to become precursor powder. Finally, the precursor was heated at 300 °C for 8 h followed by heat-treating at temperatures between 700 and 900 °C for 8 h under N$_2$ atmosphere. The compositions, crystalline structures, morphologies, carbon content, and particle size of the synthesized powder were investigated by inductive coupled plasma optical emission spectrometer (ICP-OES Optima 2100, PerkinElmer, USA), X-ray diffractometer (XRD6000, Shimadzu Corporation, Japan), scanning electron microscope (JSM-5600L, JEOL Ltd., Japan), field-emission transmission electron microscope (JEM-2100, JEOL Ltd., Japan), and element analyzer (EA, Vario EL III, Heraeus Elementar, Germany).

The synthesized materials were mixed with polyvinylidene fluoride (PVDF, Kynar 740, ELF, Germany) and acetylene black (99.99%, Strem Chemicals Inc., USA) with a weight ratio of 83:7:10 in adequate amount of N-methyl-2-pyrrolidone (NMP, ultra, ISP Technologies Inc., USA) and stirred for 1 day to become slurry. Then the slurries were coated on aluminum foil by a doctor blade coater. After drying and pressing, the tapes were punched into 10.0 mm disk electrodes. The electrodes were assembled into CR2032 coin-type cells with Li or MCMB anodes, 1 M LiPF$_6$ in EC–DEC (volume ratio of 1:1) (Tomiyama, Japan) electrolyte, and separator (Celgard 2400, Hoechst. Celanese, USA) in an argon-filled glove box. The assembled cells were used for capacity retention and cycling voltammetric studies with home-made battery tester and a potentiostat/galvanostat (Autolab PGSTAT30, Eco Chemie B.V., Netherlands) with various C rates or potential scan rates within cutoff voltages of 2.5 and 4.3 V at 30 °C.

3. Results and discussion

The compositions of the LiFePO$_4$ powders synthesized at various heat-treatment temperatures determined by ICP-OES were close to the expected stoichiometric ratio. The XRD patterns of the prepared LiFePO$_4$ samples are shown in Fig. 1(a). Olivine structure was found exclusively in the samples prepared at temperatures lower than 800 °C. In addition to the olivine phase, hexagonal Fe$_2$P can be found in samples prepared at temperatures higher than 800 °C, whereas orthorhombic Li$_3$PO$_4$ can also be observed in samples heated at temperatures higher than 850 °C, as shown in Fig. 1(b). The calculated lattice constants of olivine in the prepared samples are summarized in Table 1. Among the prepared samples, the 750 °C sample showed the largest bc value. It has been reported that
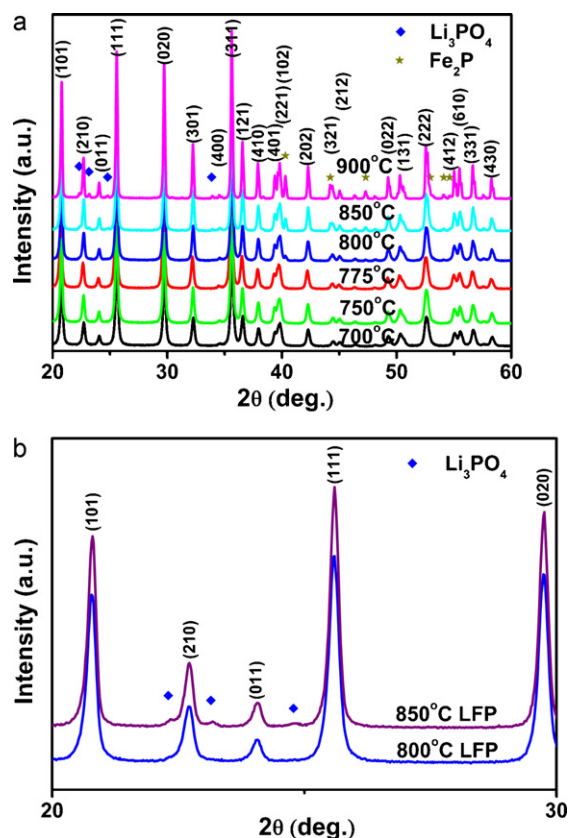

Fig. 1. (a) XRD patterns of the LiFePO$_4$ powders synthesized at various heat treatment temperatures and (b) partial enlargement of the patterns of the samples prepared at 800 and 850 °C.

LiFePO$_4$ with larger bc value could profit the electrochemical performance due to the enhancement of the diffusion path of lithium ion [19]. From the results of EA analysis listed in Table 2, it can be found that the variation of the carbon content of the prepared samples is insignificant except the 900 °C sample. It may suggest that the degree of carbon content may not play an important role on the electrochemical properties for samples prepared at temperatures lower than 850 °C.

From the SEM photographs of the prepared samples, as shown in Fig. 2, particle agglomeration can be obviously observed. The primary particle size of the prepared samples increases from 110 nm to 180 nm as the heat-treatment temperature was increased from 700 to 800 °C and becomes 300 nm in 900 °C prepared sample. That may be attributed to the grain growth of particles at high temperatures, especially for 900 °C sample. From the FEG-TEM photograph and the SAD pattern of the sample prepared at 900 °C (shown in Fig. 3), a layer of Fe$_2$P can be observed on the surface of LiFePO$_4$ particle and a value of 2.2525 Å for d_{111} of hexagonal structured Fe$_2$P was obtained by Gatan Digital-Micrograph. This value is slightly higher than the standard value of Fe$_2$P (2.2371 Å).

Table 1
Calculated lattice parameters of olivine of the LiFePO$_4$ powders synthesized at various heat-treatment temperatures.

Sample	Lattice parameter			
	a (Å)	b (Å)	c (Å)	bc (Å^2)
700 °C LiFePO$_4$	10.320(5)	6.004(1)	4.692(5)	28.17
750 °C LiFePO$_4$	10.328(9)	6.016(2)	4.681(4)	28.28
775 °C LiFePO$_4$	10.323(8)	6.005(5)	4.694(6)	28.19
800 °C LiFePO$_4$	10.324(9)	6.006(0)	4.693(6)	28.19
850 °C LiFePO$_4$	10.325(4)	6.004(8)	4.691(3)	28.17
900 °C LiFePO$_4$	10.329(4)	6.006(2)	4.691(1)	28.17

Table 2
Carbon contents of the LiFePO$_4$ powders synthesized at various heat-treatment temperatures.

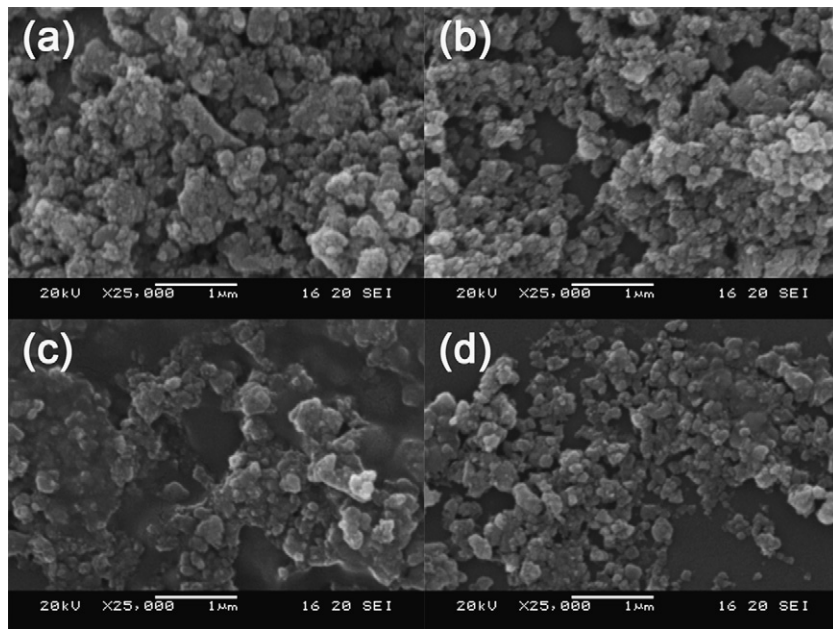| Sample	Carbon content (wt%)
700 °C LiFePO$_4$	5.05
750 °C LiFePO$_4$	5.216
775 °C LiFePO$_4$	5.224
800 °C LiFePO$_4$	5.32
850 °C LiFePO$_4$	4.656
900 °C LiFePO$_4$	4.237

Fig. 2. SEM photographs of LiFePO$_4$ samples synthesized at (a) 700 °C, (b) 750 °C, (c) 775 °C, and (d) 800 °C.

The charge/discharge curves of the second cycle of the coin-typed LiFePO$_4$/Li cells comprised LiFePO$_4$ samples synthesized at various heat-treatment temperatures are plotted in Fig. 4. All samples show characteristic charge/discharge potential plateaus of LiFePO$_4$ at 3.44 V and 3.39 V vs. Li/Li$^+$. The discharge capacities of second cycle for the LiFePO$_4$ samples synthesized at 700, 750, 775, 800, 850, and 900 °C are 145, 150, 155, 143, 136 and 91 mAh g^{-1}, respectively, as the cells were cycled with 1/10C rate. The results of the capacity retention studies for the cells comprised the prepared samples cycled with various C rates at 30 °C are shown in Fig. 5. The samples prepared at 750 and 775 °C show superior cycling performance than others because of their large bc values and the presence of small amount of Fe$_2$P though it could not be identified from the XRD patterns. Figs. 6 and 7 show the charge/discharge curves of
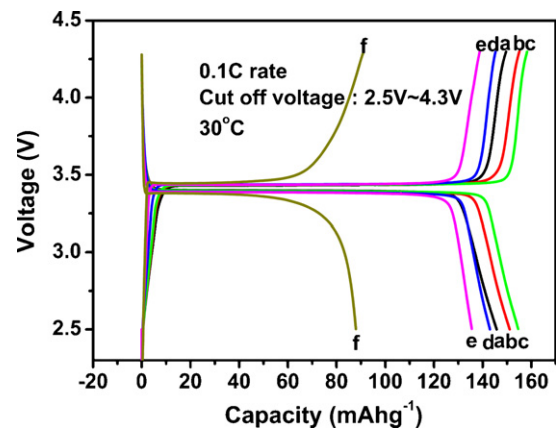

Fig. 4. Charge/discharge curves of the second cycle of the LiFePO$_4$/Li coin-typed cells comprised LiFePO$_4$ samples synthesized at (a) 700 °C, (b) 750 °C, (c) 775 °C, (d) 800 °C, (e) 850 °C, and (f) 900 °C.

the second cycle and the results of capacity retention study of the cells comprised LiFePO$_4$ sample synthesized at 775 °C. Due to the increasing capacity during the initial cycles that may be caused by the inappropriate cell assembly, the charge/discharge curves of the
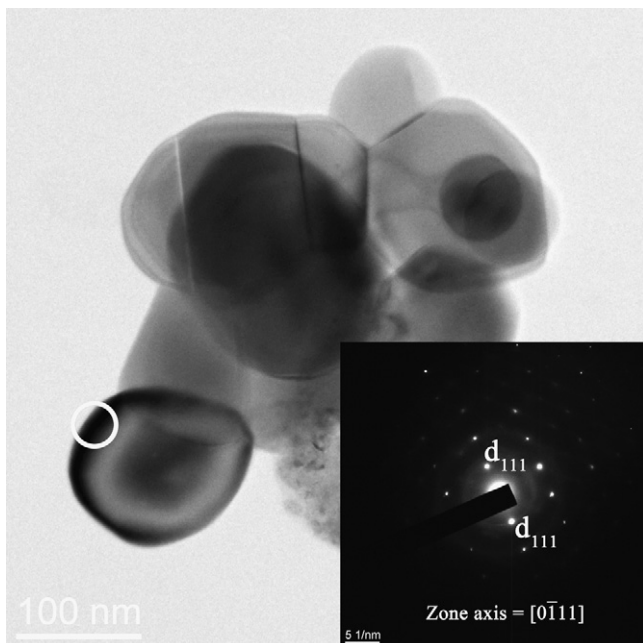

Fig. 3. FEG-TEM photograph and SAD pattern of the sample synthesized at 900 °C.
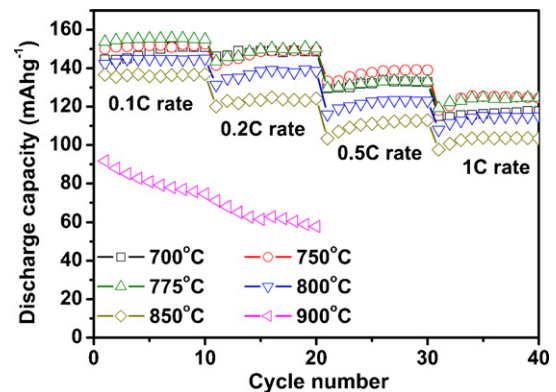

Fig. 5. Cycling performance of the LiFePO$_4$/Li coin-typed cells comprised samples synthesized at various heat-treatment temperatures.
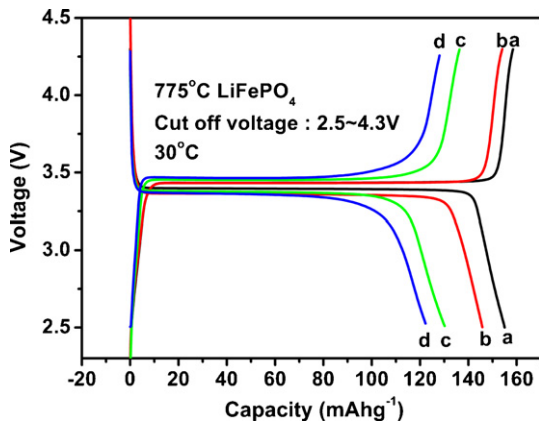
Fig. 6. Charge/discharge curves of the second cycle of the LiFePO$_4$/Li coin-typed cells comprised sample synthesized at 775 °C with (a) $C/10$, (b) $C/5$, (c) $C/2$, and (d) $1C$ rates.

Fig. 8. Cycling performance of the LiFePO$_4$/MCMB cells comprised samples synthesized at 700 and 800 °C with 0.15C rate.

second cycle are shown, and the 775 °C sample shows discharge capacities of 155, 146, 130 and 122 mAh g^{-1} as it was cycled with $C/10$, $C/5$, $C/2$, and $1C$ rates, respectively. The polarization between charge and discharge plateaus increases while the charge/discharge capacities decrease with increasing cycling rate. Several studies had reported that samples containing Fe$_2$P can improve the cycling performance and rate capability of LiFePO$_4$ materials [13,14,16–18]. However, the Fe$_2$P containing samples synthesized at temperatures higher than 800 °C in this study do not show improvement on cycling performance and rate capability. That may be attributed to the grain growth and the formation of Li$_3$PO$_4$ in the samples prepared at temperatures higher than 800 °C [13].

It had been suggested that the existence of small amount of Fe$_2$P on the surface of particles could improve the electrochemical properties of LiFePO$_4$ material [14]. For comparison, LiFePO$_4$/MCMB cells comprised samples synthesized at 700 and 800 °C were cycled with 0.15C rate at room temperature to reveal the effect of Fe$_2$P on the cycling performance of LiFePO$_4$ material. Fig. 8 shows the results of the capacity retention LiFePO$_4$/MCMB cells. The cell comprised 800 °C sample shows lower capacity fading rate than that of 700 °C sample. That may be attributed to the sample prepared at 700 °C has smaller particle size and larger specific surface area, thus higher iron ion dissolution and higher capacity fading rates than 800 °C sample. From the charge/discharge curves of the 1st, 10th, 20th, 50th, and 100th cycles of the LiFePO$_4$/MCMB cells prepared with samples synthesized at 700 and 800 °C, shown in Fig. 9, it is found that the LiFePO$_4$/MCMB cell comprised 800 °C prepared sample shows higher polarization growth rate than that of 700 °C
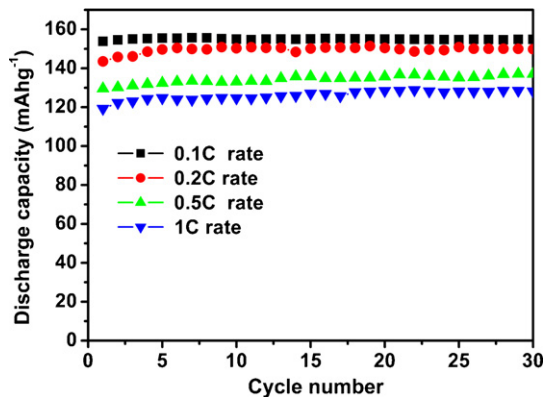
sample. That may be caused by the growth of SEI layer due to the reactions between additives and electrolyte.

Fig. 10 presents the typical cycling voltammograms of LiFePO$_4$/Li cells prepared with sample synthesized at 800 °C with various potential scan rates. Similar works were also performed for samples prepared at other temperatures. The plots of anode/cathode peak currents, i_p, of Fe^{3+}/Fe^{2+} redox couple against the square root of the potential scan rate, $v^{1/2}$, are shown in Fig. 11. A linear relationship between the peak currents and $v^{1/2}$ are found for the prepared samples. It suggests that the Li$^+$ ion intercalation/de-intercalation into/from the prepared LiFePO$_4$ materials are diffusion-limited processes. The diffusion coefficients

Fig. 9. Charge/discharge curves of the 1st, 10th, 20th, 50th and 100th cycles of the LiFePO$_4$/MCMB cells with 0.15C rate for cells comprised samples synthesized at (a) 700 °C and (b) 800 °C.

Fig. 7. Cycling performance of the LiFePO$_4$/Li coin-typed cells with various C rates for cells comprised sample synthesized at 775 °C.
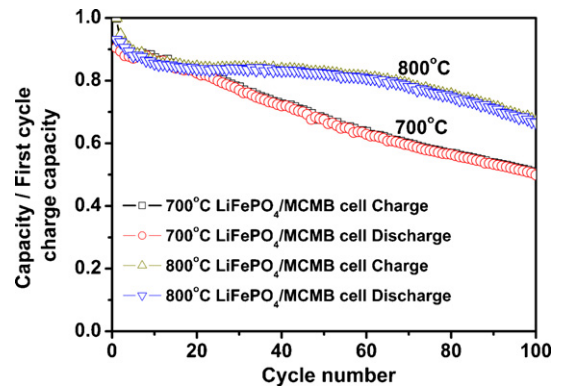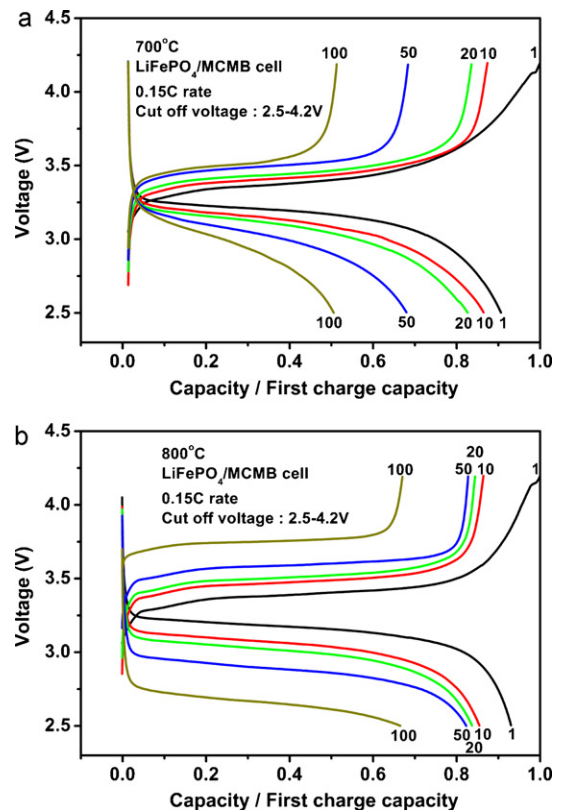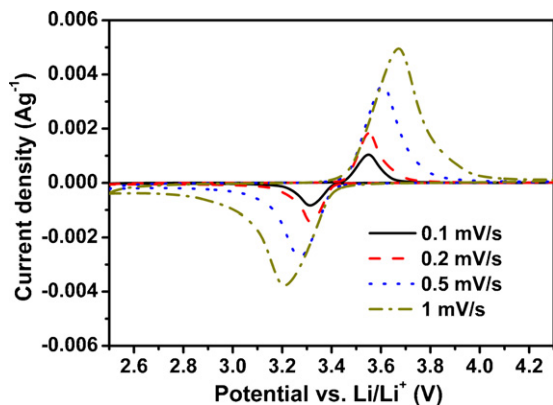
Fig. 10. Cyclic voltammograms of second cycle of the LiFePO$_4$/Li coin-typed cells comprised sample synthesized at 800 °C under various scan rates.

Table 3
Calculated diffusion coefficients of Li$^+$ ions at 30 °C for the LiFePO$_4$ materials prepared at various temperatures.

Sample	$D_{oxidation}$ (cm^2 s^{-1})	$D_{reduction}$ (cm^2 s^{-1})	$D_{average}$ (cm^2 s^{-1})
700 °C LiFePO$_4$	8.80×10^{-11}	6.36×10^{-11}	7.58×10^{-11}
750 °C LiFePO$_4$	1.79×10^{-10}	1.32×10^{-10}	1.56×10^{-10}
775 °C LiFePO$_4$	1.49×10^{-10}	9.24×10^{-11}	1.21×10^{-10}
800 °C LiFePO$_4$	1.85×10^{-10}	1.06×10^{-10}	1.46×10^{-10}
850 °C LiFePO$_4$	2.05×10^{-10}	1.11×10^{-10}	1.58×10^{-10}
900 °C LiFePO$_4$	3.52×10^{-12}	7.92×10^{-12}	5.72×10^{-12}

of Li$^+$ ion can be calculated from the relationship between i_p and $v^{1/2}$ shown as follows:

$$i_p = 0.4463 nFAC \left(\frac{nF}{RT} \right)^{1/2} D^{1/2} v^{1/2} K(\Lambda, \alpha)$$

where n is the number of electron transferred in the process, F is the Faraday constant (96500), A is the surface area of cathode electrode contacts with electrolyte (about 1600 cm^2), C is the concentration of lithium ion, D is the diffusion coefficient, and $K(\Lambda, \alpha)$ is 1 for a
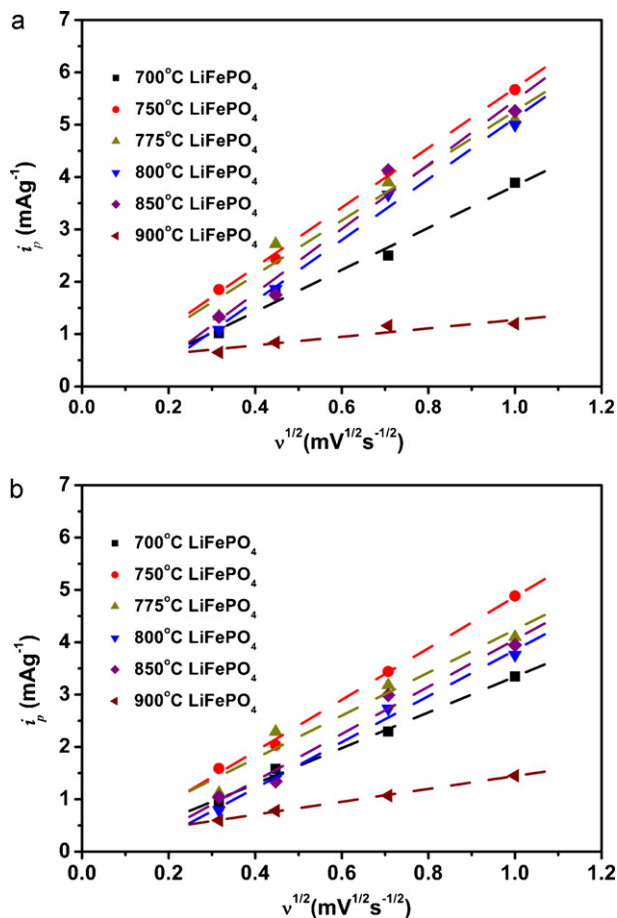
reversible reaction [20]. From the slopes shown in Fig. 11, the diffusion coefficients of Li$^+$ ion during oxidation, $D_{oxidation}$ and reduction, $D_{reduction}$ can be calculated and summarized in Table 3. It can be found that 750 °C synthesized sample shows higher Li$^+$ ions diffusion coefficient than others except 850 °C sample. It can be due to the 750 °C sample exhibits larger lattice parameters than others. However, for samples prepared at temperature between 775 and 850 °C, Li$^+$ ions diffusion coefficient increase with increasing amount of Fe$_2$P additive. The sample synthesized at 850 °C shows even higher Li$^+$ ions diffusion coefficient than that of 750 °C sample. It may be caused by the formation of a defect structure of LiFePO$_4$ that can enhance the Li$^+$ ion diffusion due to the formation of Fe$_2$P and Li$_3$PO$_4$ additives. However, the effects of formation of Fe$_2$P and Li$_3$PO$_4$ additives on Li$^+$ motion in LiFePO$_4$ are still unclear. For the sample synthesized at 900 °C, a layer of Fe$_2$P formed on the surface of LiFePO$_4$ particle, as shown in Fig. 3, which might hinder the transportation of Li$^+$ and result in the low Li$^+$ ion diffusion coefficient. These results are similar to those reported by Song et al. [21]. They suggested that there is a critical concentration of Fe$_2$P, and LiFePO$_4$ sample with Fe$_2$P can improve the rate capability and cycling behavior within the critical concentration, while LiFePO$_4$ sample with Fe$_2$P content above the critical concentration will give much more poor cycling performance.

4. Conclusions

Olivine structured LiFePO$_4$ samples were successfully synthesized via a solution method. From the XRD patterns of the prepared samples, LiFePO$_4$ sample containing Fe$_2$P can be obtained by heat-treating the stoichiometric precursor at temperatures higher than 800 °C, while Li$_3$PO$_4$ is also found in samples heat-treated at temperatures higher than 850 °C. Samples synthesized at 750 and 775 °C show the most promising cycling performance among the prepared powders. That may be attributed to the 750 °C sample has the largest bc value and thus 775 °C sample contains small amount of Fe$_2$P. Samples prepared at temperatures higher than 800 °C show worse cycling performance than 750 and 775 °C samples due to the existence of Li$_3$PO$_4$ and larger particle size than 775 °C sample. LiFePO$_4$/MCMB cell comprised 850 °C sample shows lower capacity fading rate than that assembled with 700 °C sample due to the larger particle size. However, it shows high polarization growth rate that might be caused by the reactions between the additives and electrolyte. For the samples containing Fe$_2$P, Li$^+$ ion diffusion coefficient increases with increasing temperature of heat-treatment and increasing amount of Fe$_2$P except 900 °C synthesized sample. That may be caused by the formation of defect structure of LiFePO$_4$ due to the formation of Fe$_2$P and Li$_3$PO$_4$ additives which can enhance the diffusion of Li$^+$ ions. Layers of Fe$_2$P on the surface of LiFePO$_4$ particles may hinder the diffusion of Li$^+$ ions.

Fig. 11. Plots of peak current of Fe^{3+}/Fe^{2+} redox couple of the cyclic voltammograms performed with various scan rates against the square root of scan rate, $v^{1/2}$, (a) cathodic currents and (b) anodic currents, for samples prepared at various temperatures.

References

[1] A.K. Padhi, K.S. Nanjundaswamy, C. Masquelier, S. Okada, J.B. Goodenough, J. Electrochem. Soc. 144 (1997) 1609.
[2] A.S. Andersson, J.O. Thomas, J. Power Sources 97/98 (2001) 498.
[3] N. Ravet, Y. Chouinard, J.F. Magnan, S. Besner, M. Gauthier, M. Armand, J. Power Sources 97/98 (2001) 503.
[4] P.P. Prosini, D. Zane, M. Pasquali, Electrochim. Acta 46 (2001) 3517.
[5] H. Huang, S.C. Yin, L.F. Nazar, Electrochem, Solid State Lett. 4 (2001) 170.
[6] Z. Chen, J.R. Dahn, J. Electrochem. Soc. 149 (2002) 1184.
[7] A. Yamada, S.C. Chung, K. Hinokuma, J. Electrochem. Soc. 148 (2001) 224.
[8] S.Y. Chung, J.T. Bloking, Y.M. Chiang, Nat. Mater. 1 (2002) 123.
[9] S. Shi, L. Liu, C. Ouyang, D.S. Wang, Z. Wang, L. Chen, X. Huang, Phys. Rev. B 68 (2003) 195108.
[10] D. Wang, H. Li, S. Shi, X. Huang, L. Chen, Electrochim. Acta 50 (2005) 2955.
[11] S.-H. Wu, M.-S. Chen, C.-J. Chien, Y.-P. Fu, J. Power Sources 189 (2009) 440.
[12] Y.H. Rho, L.F. Nazar, L. Perry, D. Ryan, J. Electrochem. Soc. 154 (2007) 283.
[13] Y.-W. Hu, I.D. Raistrick, R.A. Huggins, J. Electrochem. Soc. 124 (1977) 1240.
[14] Y. Kadoma, J.-M. Kim, K. Abiko, K. Ohtsuki, K. Ui, N. Kumagai, Electrochim. Acta 55 (2010) 1034.
[15] P.S. Herle, B. Ellis, N. Coombs, L.F. Nazar, Nat. Mater. 3 (2004) 147.
[16] Y. Xu, Y. Lu, L. Yan, Z. Yang, R. Yang, J. Power Sources 160 (2006) 570.
[17] W.C. Kim, J.S. Park, K.S. Lee, J. Power Sources 163 (2006) 144.
[18] M. Konarova, I. Taniguchi, J. Power Sources 194 (2009) 1029.
[19] J.M. Tarascon, M. Armand, Nature 414 (2001) 359.
[20] M. Takahashi, S.-I. Tobishima, K. Takei, Y. Sakurai, Solid State Ionics 148 (2002) 283.
[21] M.-S. Song, D.-Y. Kim, Y.-M. Kang, Y.-I. Kim, J.-Y. Lee, H.-S. Kwon, J. Power Sources 180 (2008) 546.